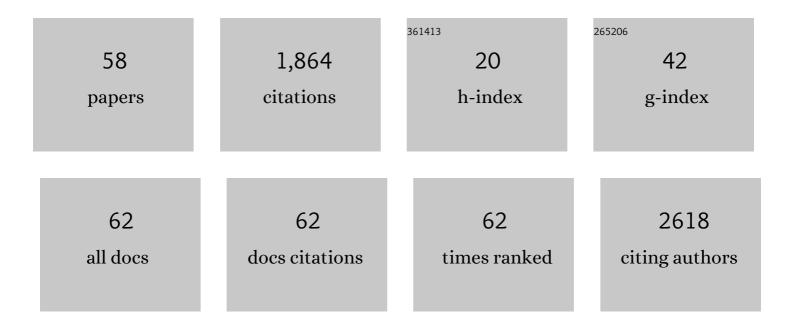
Taylor J Woehl

List of Publications by Year in descending order

Source: https://exaly.com/author-pdf/4311358/publications.pdf Version: 2024-02-01



ΤλνιορΙΜοεμι

#	Article	IF	CITATIONS
1	Real-time imaging of metallic supraparticle assembly during nanoparticle synthesis. Nanoscale, 2022, 14, 312-319.	5.6	2
2	Chemically fueled assembly of protein hydrogels driven by a redox cycle. Biophysical Journal, 2022, 121, 151a.	0.5	0
3	Visualizing Ligand-Mediated Bimetallic Nanocrystal Formation Pathways with <i>in Situ</i> Liquid-Phase Transmission Electron Microscopy Synthesis. ACS Nano, 2021, 15, 2578-2588.	14.6	25
4	pH-Mediated Aggregation-to-Separation Transition for Colloids Near Electrodes in Oscillatory Electric Fields. Langmuir, 2021, 37, 9346-9355.	3.5	7
5	Metal Ionâ€Induced Assembly of MXene Aerogels via Biomimetic Microtextures for Electromagnetic Interference Shielding, Capacitive Deionization, and Microsupercapacitors. Advanced Energy Materials, 2021, 11, 2101494.	19.5	61
6	Visualizing non-classical formation pathways of alloyed nanocrystals with liquid phase transmission electron microscopy. Microscopy and Microanalysis, 2021, 27, 2634-2635.	0.4	0
7	Investigating electron beam interactions with nanoparticle capping ligands using correlative liquid phase transmission electron microscopy and fluorescence microscopy. Microscopy and Microanalysis, 2021, 27, 2624-2625.	0.4	0
8	Revealing Reactions between the Electron Beam and Nanoparticle Capping Ligands with Correlative Fluorescence and Liquid-Phase Electron Microscopy. ACS Applied Materials & Interfaces, 2021, 13, 37553-37562.	8.0	15
9	Probing Electron Beam – Nanoparticle Capping Ligand Interactions during Liquid Phase Transmission Electron Microscopy Using a Correlative Fluorescence Microscopy Assay. Microscopy and Microanalysis, 2021, 27, 21-22.	0.4	0
10	Detection and Sizing of Submicron Particles in Biologics With Interferometric Scattering Microscopy. Journal of Pharmaceutical Sciences, 2020, 109, 881-890.	3.3	4
11	Effects of Protein Unfolding on Aggregation and Gelation in Lysozyme Solutions. Biomolecules, 2020, 10, 1262.	4.0	10
12	Metal Nanocrystal Formation during Liquid Phase Transmission Electron Microscopy: Thermodynamics and Kinetics of Precursor Conversion, Nucleation, and Growth. Chemistry of Materials, 2020, 32, 7569-7581.	6.7	22
13	Electron-beam-driven chemical processes during liquid phase transmission electron microscopy. MRS Bulletin, 2020, 45, 746-753.	3.5	38
14	Probing the Surface Structure of Monoclonal Antibody Aggregates with Multiscale Microscopy. Microscopy and Microanalysis, 2020, 26, 1068-1069.	0.4	0
15	Establishing Flask-Relevant Reaction Conditions for Imaging Bimetallic Nanocrystal Formation with Liquid Phase Transmission Electron Microscopy. Microscopy and Microanalysis, 2020, 26, 2568-2570.	0.4	0
16	A Fluorescence Microscopy Assay for Assessing Beam Damage to Nanoparticle Capping Ligands During Liquid Cell Electron Microscopy. Microscopy and Microanalysis, 2019, 25, 1672-1673.	0.4	1
17	Nanoscale Mapping of Nonuniform Heterogeneous Nucleation Kinetics Mediated by Surface Chemistry. Journal of the American Chemical Society, 2019, 141, 13516-13524.	13.7	29
18	Visualizing Platinum Supraparticle Formation with Liquid Cell Electron Microscopy and Correlative Investigation of Catalytic Activity. Microscopy and Microanalysis, 2019, 25, 2026-2027.	0.4	0

TAYLOR J WOEHL

#	Article	IF	CITATIONS
19	Structurally colored protease responsive nanoparticle hydrogels with degradation-directed assembly. Nanoscale, 2019, 11, 17904-17912.	5.6	6
20	Irreversible Nature of Mesoscopic Aggregates in Lysozyme Solutions. Colloid Journal, 2019, 81, 546-554.	1.3	8
21	Quantification of rhenium oxide dispersion on zeolite: Effect of zeolite acidity and mesoporosity. Journal of Catalysis, 2019, 372, 128-141.	6.2	16
22	Toward Quantitative Liquid Cell Electron Microscopy through Kinetic Control of Solution Chemistry. Microscopy and Microanalysis, 2019, 25, 23-24.	0.4	2
23	Refocusing <i>in Situ</i> Electron Microscopy: Moving beyond Visualization of Nanoparticle Self-Assembly To Gain Practical Insights into Advanced Material Fabrication. ACS Nano, 2019, 13, 12272-12279.	14.6	10
24	Mesopore differences between pillared lamellar MFI and MWW zeolites probed by atomic layer deposition of titania and consequences on photocatalysis. Microporous and Mesoporous Materials, 2019, 276, 260-269.	4.4	11
25	Effects of substrate porosity in carbon aerogel supported copper for electrocatalytic carbon dioxide reduction. Electrochimica Acta, 2019, 297, 545-552.	5.2	24
26	Direct Visualization of Planar Assembly of Plasmonic Nanoparticles Adjacent to Electrodes in Oscillatory Electric Fields. Langmuir, 2018, 34, 6237-6248.	3.5	5
27	Utilizing Electron Beam Control and Radiation Chemistry during Liquid Cell Electron Microscopy to Image Protein Aggregates in their Native Hydrated State. Microscopy and Microanalysis, 2018, 24, 1976-1977.	0.4	0
28	Quantitative Modeling of Kinetically Controlled Nanocrystal Synthesis with Liquid Cell Electron Microscopy. Microscopy and Microanalysis, 2018, 24, 280-281.	0.4	0
29	Quantifying the Nucleation and Growth Kinetics of Electron Beam Nanochemistry with Liquid Cell Scanning Transmission Electron Microscopy. Chemistry of Materials, 2018, 30, 7727-7736.	6.7	61
30	Directional Statistics of Preferential Orientations of Two Shapes in Their Aggregate and Its Application to Nanoparticle Aggregation. Technometrics, 2018, 60, 332-344.	1.9	5
31	Multi-Component Fe–Ni Hydroxide Nanocatalyst for Oxygen Evolution and Methanol Oxidation Reactions under Alkaline Conditions. ACS Catalysis, 2017, 7, 365-379.	11.2	154
32	Nature of peptide wrapping onto metal nanoparticle catalysts and driving forces for size control. Nanoscale, 2017, 9, 8401-8409.	5.6	29
33	Control of Radiation Chemistry during Liquid Cell TEM to Synthesize Transition Metal and Bimetallic Nanoparticles. Microscopy and Microanalysis, 2017, 23, 854-855.	0.4	0
34	Correlative in situ Analysis of Magnetosome Magnetite Biomineralization. Microscopy and Microanalysis, 2016, 22, 12-13.	0.4	0
35	Toward a modular multi-material nanoparticle synthesis and assembly strategy via bionanocombinatorics: bifunctional peptides for linking Au and Ag nanomaterials. Physical Chemistry Chemical Physics, 2016, 18, 30845-30856.	2.8	10
36	Dark-field image contrast in transmission scanning electron microscopy: Effects of substrate thickness and detector collection angle. Ultramicroscopy, 2016, 171, 166-176.	1.9	8

TAYLOR J WOEHL

#	Article	IF	CITATIONS
37	Peptide-Directed PdAu Nanoscale Surface Segregation: Toward Controlled Bimetallic Architecture for Catalytic Materials. ACS Nano, 2016, 10, 8645-8659.	14.6	58
38	Dark-Field Scanning Transmission Ion Microscopy via Detection of Forward-Scattered Helium Ions with a Microchannel Plate. Microscopy and Microanalysis, 2016, 22, 544-550.	0.4	16
39	The Mechanisms for Preferential Attachment of Nanoparticles in Liquid Determined Using Liquid Cell Electron Microscopy, Machine Learning, and Molecular Dynamics. Microscopy and Microanalysis, 2016, 22, 812-813.	0.4	1
40	Harnessing Control of Radiolysis during Liquid Cell Electron Microscopy to Enable Visualization of Nanomaterial Transformation Dynamics. Microscopy and Microanalysis, 2016, 22, 40-41.	0.4	3
41	Understanding the Role of Solvation Forces on the Preferential Attachment of Nanoparticles in Liquid. ACS Nano, 2016, 10, 181-187.	14.6	51
42	An Analytical Scattering Model for Low Energy Annular Dark Field Transmission Scanning Electron Microscopy. Microscopy and Microanalysis, 2015, 21, 1263-1264.	0.4	0
43	Visualization of Gold Nanoparticle Self-assembly Kinetics. Microscopy and Microanalysis, 2015, 21, 945-946.	0.4	0
44	Correlative Electron and Fluorescence Microscopy of Magnetotactic Bacteria in Liquid: Toward In Vivo Imaging. Microscopy and Microanalysis, 2015, 21, 1499-1500.	0.4	1
45	The Mechanisms for Nanoparticle Surface Diffusion and Chain Self-Assembly Determined from Real-Time Nanoscale Kinetics in Liquid. Journal of Physical Chemistry C, 2015, 119, 21261-21269.	3.1	86
46	Minimum Cost Multi-Way Data Association for Optimizing Multitarget Tracking of Interacting Objects. IEEE Transactions on Pattern Analysis and Machine Intelligence, 2015, 37, 611-624.	13.9	60
47	Visualization of Iron-Binding Micelles in Acidic Recombinant Biomineralization Protein, MamC. Journal of Nanomaterials, 2014, 2014, 1-7.	2.7	15
48	Direct Observation of Aggregative Nanoparticle Growth: Kinetic Modeling of the Size Distribution and Growth Rate. Nano Letters, 2014, 14, 373-378.	9.1	172
49	Electrolyte-Dependent Aggregation of Colloidal Particles near Electrodes in Oscillatory Electric Fields. Langmuir, 2014, 30, 4887-4894.	3.5	34
50	Nucleation of Iron Oxide Nanoparticles Mediated by Mms6 Protein <i>in Situ</i> . ACS Nano, 2014, 8, 9097-9106.	14.6	90
51	Correlative Fluorescence and Liquid Cell STEM of Live Magnetotactic Bacteria. Microscopy and Microanalysis, 2014, 20, 1510-1511.	0.4	1
52	Protein-Mediated Nucleation of Nanoparticles In-Situ. Microscopy and Microanalysis, 2014, 20, 1604-1605.	0.4	0
53	Direct Observation of Aggregative Nanoparticle Growth: Kinetic Modeling of the Size Distribution and Growth Rate. Microscopy and Microanalysis, 2014, 20, 1612-1613.	0.4	0
54	Implementing in situ Experiments in Liquids in the (Scanning) Transmission Electron Microscope ((S)TEM) and Dynamic TEM (DTEM). Microscopy and Microanalysis, 2014, 20, 1648-1649.	0.4	1

TAYLOR J WOEHL

#	Article	IF	CITATIONS
55	Correlative Electron and Fluorescence Microscopy of Magnetotactic Bacteria in Liquid: Toward In Vivo Imaging. Scientific Reports, 2014, 4, 6854.	3.3	65
56	Experimental procedures to mitigate electron beam induced artifacts during in situ fluid imaging of nanomaterials. Ultramicroscopy, 2013, 127, 53-63.	1.9	176
57	Direct <i>in Situ</i> Observation of Nanoparticle Synthesis in a Liquid Crystal Surfactant Template. ACS Nano, 2012, 6, 3589-3596.	14.6	93
58	Direct <i>in Situ</i> Determination of the Mechanisms Controlling Nanoparticle Nucleation and Growth. ACS Nano, 2012, 6, 8599-8610.	14.6	378